High-pressure new phases of V–N compounds

Xu-Han Shi(时旭含)[1,2], Zhi-Hui Li(李志慧)[1], Yuanyuan Liu(刘媛媛)[1], Yuanyuan Wang(王元元)[1], Ran Liu(刘冉)[1], Kuo Hu(胡阔)[1,†], and Zhen Yao(姚震)[1,‡]

[1] *Synergetic Extreme Condition High-Pressure Science Center, State Key Laboratory of Superhard Materials, College of Physics, Jilin University, Changchun* 130012, *China*
[2] *Aviation University of Air Force, Changchun* 130022, *China*

(Received 3 October 2022; revised manuscript received 12 February 2023; accepted manuscript online 16 February 2023)

The high-pressure diagram of V–N compounds is enriched by proposed seven new stable high-pressure phases. The *P*-1-VN_4 with the armchair N-rich structure may be quenched to ambient conditions. The formed N–N covalent bond plays an important role for the structural stability of N-chain. The charge transfer results in a V–N ionic bond interaction, which further improves the stability of N-chain structure. The *P*-1-VN_4, *P*4*mnc*-VN_8, and *Immm*-VN_{10} with the outstanding detonation properties have potential application in explosive field.

Keywords: high-pressure, N-rich V–N compounds, phase diagram, stability, DFT calculation

PACS: 61.50.–f, 31.15.E–, 81.40.Vw, 52.77.Fv **DOI:** 10.1088/1674-1056/acbc6d

1. Introduction

As the huge development of society and the shortage of traditional energy materials, exploiting the new materials with high energy density is important to meet the increasing energy demand. The nitrogen atom with five valence electrons ($2s^2 2p^3$) has rich bonding forms, such as N–N single bond, N=N double bond, and N≡N triple bond. At ambient conditions, nitrogen exists in the form of triple bonded diatomic molecules (N_2). Under high pressure, as the distance between molecules (N_2) reducing, the N≡N triple bond gradually dissociates and rebonds to a new polymeric nitrogen phase with the single or double bond form. Due to the large energy difference between the triple bond and the single/double bonds, polymeric nitrogen can release a large amount of bond energy when dissociate to the gaseous N_2. For example, the energy density of well-known *cg*-N is as high as 9.7 kJ/g, which is much higher than that of TNT (4.3 kJ/g) and HMX (5.7 kJ/g). Most importantly, the dissociation product N_2 is pollution-free. Thus, polymeric nitrogen with the high energy density and environmentally friendly properties is expected to play a great role in the applications of energy storage and new explosives.

Intensive theoretical and experimental efforts have focused on the designing and synthesizing the polymeric nitrogen structures. In theory, a variety of polymeric nitrogen structures have been proposed, such as the molecular phases (N_2–N_6, N_8, N_{10}, N_{11}, N_{12}),[1–4] the layered structures (*BP*, *LP*, *HLP*, *A*7, *CH*, *LB*, *ZS*, *Cmcm*),[5–7] the network structures (*cg*-N, *PP*, *CW*, *Pba*2),[8–12] and the cage-like structures (N_{10}).[13] In experiment, four polymeric nitrogen structures were successfully synthesized at high temperature and high pressure conditions, such as the *cg*-N ($P = 110$ GPa, $T = 2000$ K)[14] and two-dimensional layered *BP*-N (140 GPa, 4000 K), *LP*-N ($P = 150$ GPa, $T = 3000$ K), and *HLP*-N ($P = 244$ GPa, $T = 3300$ K).[15–17] In decompression studies, the *cg*-N, *BP*-N, *LP*-N, and *HLP*-N can be quenched to 42 GPa, 48 GPa, 52 GPa, and 66 GPa, respectively.

In view of the harsh synthetic conditions and the low stability of polymeric nitrogen, people are eager to find a way to overcome the shortcomings of polymeric nitrogen and realize the practical application of polymeric nitrogen as soon as possible. Recent studies found that the "chemical pre-compression" effect by introducing the coordination elements can induce novel polynitrogen structures, which may possess the milder synthesis conditions and higher stability than that of pure solid nitrogen. For example, a variety of polynitrogen structures with the different construction units are found in theory, such as the infinite polymeric N-chains in MN_4 ($M =$ Be, Mg, Ca, Sr, and Mn),[18–24] the N_5 ring in MN_5 ($M =$ Li, Na, K, Rb, and Cs),[25–29] the N_6 ring in MN_3 ($M =$ Li, Na, K, Rb, and Cs),[30–33] and MN_6 ($M =$ Ba, Mo, W, and Re),[34–37] the N-layer in K_2N_{16}, BeN_4, CoN_8, and CdN_6,[19,38–40] and network structures in ScN_5 and HeN_4.[41,42] Experimentally, pentazolate N_5 structures in LiN_5 and CsN_5 have been synthesized successfully at 45 GPa and 65 GPa, which are significantly lower than that of *cg*-N (110 GPa).[43,44] Moreover, the LiN_5 and CsN_5 can be quenched to ambient conditions and 18 GPa, respectively. Hence, introducing the coordination element is a very good method for reducing the formation conditions and improving the stability of polymeric nitrogen structures.[45–47]

Transition metal nitrides have attracted extensive atten-

†Corresponding author. E-mail: hukuo@jlu.edu.cn
‡Corresponding author. E-mail: yaozhen@jlu.edu.cn

© 2023 Chinese Physical Society and IOP Publishing Ltd

tion due to their excellent properties, such as high bulk elastic modulus, excellent thermal stability and electrical conductivity. Several studies have been performed to explore the novel polynitrogen structures by applying the transition metal as the coordination elements. For example, the *Immm*-HfN_{10} with the armchair polymeric N-chains has been reported in theory.[48] The FeN_4 with the infinite polymeric N-chain structure has been successfully synthesized by heating Fe and N_2 at 106 GPa in experiment.[49] As is well known, the selection of coordination element is important for the construction of the polynitrogen structures. Vanadium (V) with the low molar mass in the transition metal group and the abundant valence electrons ($3p^6 3d^4 4s^1$) is considered to be an ideal coordination element for the construction of novel polynitrogen structures. The vanadium nitride (VN) has been widely used in rigid materials, coatings and superconducting components industrial fields due to its excellent properties of hardness, thermal stability and superconductivity (T_C = 2 K–9 K). Under ambient pressure, *P*-31*m*-VN_2 structure exhibits an outstanding Vickers hardness (H_V = 35.6 GPa), which is much higher than that of the reported high-hardness materials, such as the ZrN_2 (H_V = 26.4 GPa), and HfN_2 (H_V = 27.6 GPa).[50] Up to now, the reported V–N compounds are all focus on the low nitrogen content structures. Thus, it is necessary to explore the N-rich V–N compounds for probing the novel structures and properties.

2. Computation details

The theoretical prediction is performed by using the particle swarm optimization structure prediction algorithm (CALYPSO software).[51] Ten stoichiometric ratios of VN_x (x = 1/2, 1, 2, 3, 4, 5, 6, 7, 8, 10) are considered in the structural search. The crystal structure is predicted under four prediction pressures (P = 0 GPa, 20 GPa, 50 GPa, and 100 GPa). The simulation cells of VN_x contain 1, 2, and 4 formula units (f.u.). The generalized gradient approximation (GGA) with the Perdew–Burke–Ernzerhof (PBE) exchange–correlation function is applied in the DFT calculation.[52] The energy cutoff for plane wave basis is set to 520 eV. The electron configurations of $3p^6 3d^4 4s^1$ for V and $2s^2 2p^3$ for N are treated as valence states. The Monkhorst–Pack k-mesh spacing is $2\pi \times 0.03$ Å^{-1} in the structural optimization and the calculations of electronic structure properties. The structural formation enthalpies (ΔH_f) are calculated by using the fractional representation $\Delta H_f(VN_x) = [H(VN_x) - (1-)H(V) - xH(N)]$ ($0 < x < 1$). The phonon dispersion curves are carried out by finite displacement approach in the PHONOPY code. The *ab initio* molecular dynamics simulation (AIMD) adopts the *NVT* ensemble (constant number of atoms N, volume V, and constant temperature T). The total simulation time with the time steps of 1 fs is 10 ps. The temperature of simulated system is controlled by the Nose thermostat. The detonation velocity and detonation pressure have been calculated by using the Kamlet–Jacobs simi-empirical equation: $V_d = 1.01(NM^{0.5}E_d^{0.5})^{0.5}(1 + 1.30\rho)$ and $P_d = 15.58\rho^2 NM^{0.5}E_d^{0.5}$. N represents the moles of gas per gram of VN_x, M represents the average molar mass of gas products, E_d is the detonation chemical energy, and ρ is the mass density.[39,40,53]

3. Results and discussion

The formation enthalpies (ΔH^f) of energetically favorable VN_x phases and their phase diagrams are presented in Fig. 1.

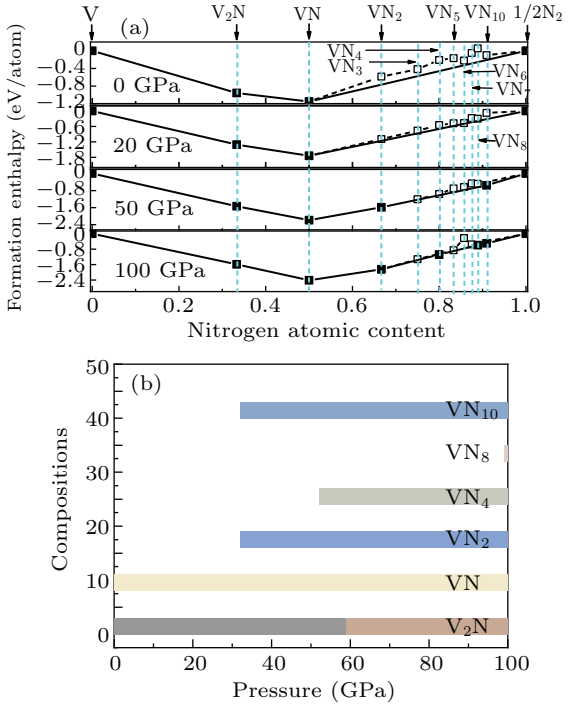


Fig. 1. (a) The formation enthalpies of VN phases with vanadium and 1/2 nitrogen at different pressures. (b) The phase diagram of predicted V–N compounds.

On the convex hull, the solid squares denote the thermodynamically stable phases, while the blank squares denote the metastable/unstable phases. For the V_2N stoichiometry, the *Pbcn*- and *Pnnm*-V_2N phases are proposed at 0 GPa/20 GPa and 50 GPa/100 GPa, respectively (Fig. 1(a)). The phase transformation pressure between *Pbcn*- and *Pnnm*-V_2N phases is 59 GPa (Fig. 1(b) and Fig. S1(a) in the supporting information). At considered four pressures, we predicted the *P*-6*m*2-VN phase, for which the stable pressure ranges from 0 GPa to 100 GPa. The *I*4*mcm*-VN_2 is found at predicted pressures of 50 GPa and 100 GPa. The stable pressure range is 32 GPa–100 GPa (Fig. 1(b) and Fig. S1(b)). At 100 GPa, we proposed the *P*-1-VN_4 and *P*4*mnc*-VN_8, for which the stable pressure ranges are 52 GPa–100 GPa and 99 GPa–100 GPa, respectively (Fig. 1(b) and Figs. S1(c) and S1(d)). At 50 GPa and 100 GPa, we predicted the *Immm*-VN_{10}, which is stable at the pressure range of 32 GPa–100 GPa (Figs. 1(b) and Fig. S1(e)).

For the presented crystal structures of predicted seven V–N compounds in Fig. 2, we can see that no polymeric nitrogen structures are formed in the *Pbcn*-V_2N and *Pnnm*-V_2N and *P*-6*m*2-VN phases. The diatomic N_2 structure is formed in *I*4*mcm*-VN_2. As the nitrogen content increase, the armchair N-chain structures are formed in *P*-1-VN_4, *P*4*mnc*-VN_8, and *Immm*-VN_{10} phases.

To further confirm the stability of predicted high-pressure phases, we performed the calculations of the phonon dispersion curves and elastic constants. As shown in Fig. 3, the *P*-1-VN_4, *P*4*mnc*-VN_8, and *Immm*-VN_{10} possess the dynamics stability at their predicted pressures due to that no imaginary frequency is observed over the Brillouin zone. Similarly, the low nitrogen content structures (*Pbcn*-V_2N, *Pnnm*-V_2N, *P*-6*m*2-VN, *I*4/*mcm*-VN_2) also possess the dynamical stability at their predicted pressures as the presented phonon dispersion curves in Fig. S2. The elastic constants of *Pbcn*-V_2N, *Pnnm*-V_2N, *P*-6*m*2-VN, *I*4/*mcm*-VN_2, *P*4*mnc*-VN_8, and *Immm*-VN_{10} are presented in Table 1. For the monoclinic phase *P*-1-VN_4, the elastic constants are presented in Table 2. According to the presented stability criteria of tetragonal, orthorhombic, hexagonal and monoclinic phases in Supporting information, we can see that the elastic constants of *Pbcn*-V_2N, *Pnnm*-V_2N, *P*-6*m*2-VN, 4/*mcm*-VN_2, *P*-1-VN_4, *P*4*mnc*-VN_8, and *Immm*-VN_{10} are all satisfy the stability criteria, indicating that they are mechanically stable. Thus, the obtained seven V–N compounds are the stable high-pressure phases.

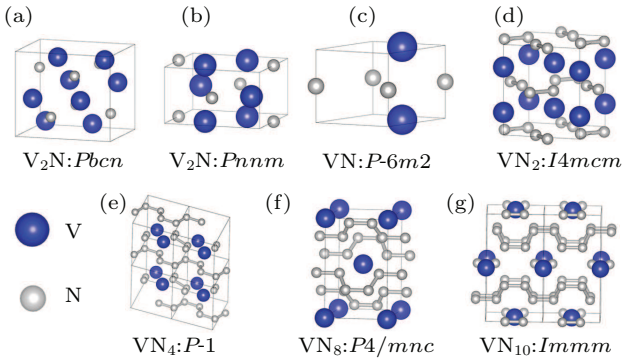


Fig. 2. The structures of V–N compounds: (a) *Pbcn*-V_2N, (b) *Pnnm*-V_2N, (c) *P*-6*m*2-VN, (d) *I*4/*mcm* VN_2, (e) *P*-1-VN_4, (f) *P*4*mnc*-VN_8, and (g) *Immm*-VN_{10}.

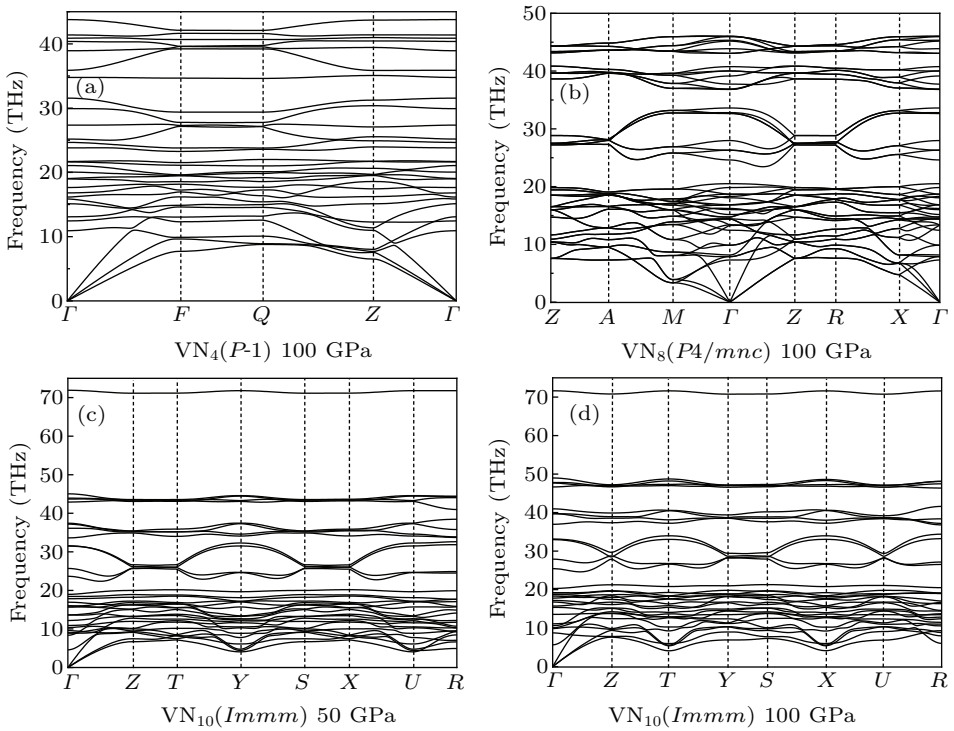


Fig. 3. Phonon dispersion curves of (a) *P*-1-VN_4 at 100 GPa, (b) *P*4*mnc*-VN_8 at 100 GPa, and [(c) and (d)] *Immm*-VN_{10} at 50 GPa and 100 GPa.

Table 1. The elastic constants C_{ij} (in unit GPa) of *Pbcn*-V_2N, *Pnnm*-V_2N, *P*-6*m*2-VN, *I*4/*mcm*-VN_2, *P*4*mnc*-VN_8, and *Immm*-VN_{10} at high pressures.

VN_x	Pressure (GPa)	C_{11}	C_{22}	C_{33}	C_{44}	C_{55}	C_{66}	C_{12}	C_{13}	C_{23}
Pbcn-V_2N	0	425.8	478.71	460.27	145.19	157.42	155.34	189.02	186.05	164.22
Pnnm-V_2N	50	631.61	766.23	640.77	197.22	165.14	271.25	301.17	299.59	258.52
P-6*m*2-VN	0	663.93	–	903.94	276.42	–	–	187.92	146.53	–
*I*4/*mcm*-VN_2	50	963.17	–	882.75	314.55	–	–	294.08	262.14	–
*P*4*mnc*-VN_8	100	530.34	–	1512.69	145.02	–	–	425.72	186.98	–
Immm-VN_{10}	50	653.99	1054.71	773.21	242.01	232.91	123.02	253.98	219.62	219.62

Table 2. The elastic constants C_{ij} (in unit GPa) of the *P*-1-VN_4 at high pressures.

P-1-VN_4 (100 GPa)	C_{11}	C_{22}	C_{33}	C_{44}	C_{55}	C_{66}	C_{12}	C_{13}	C_{14}	C_{15}	C_{16}
	1028.82	1297.7	771.55	324.56	353.15	350.58	289.7	331.21	14.6	131.51	12.81
		C_{23}	C_{24}	C_{25}	C_{26}	C_{34}	C_{35}	C_{36}	C_{45}	C_{46}	C_{56}
		317.88	8.95	58.40	37.5	1.06	–25.39	19.75	24.22	63.42	4.69

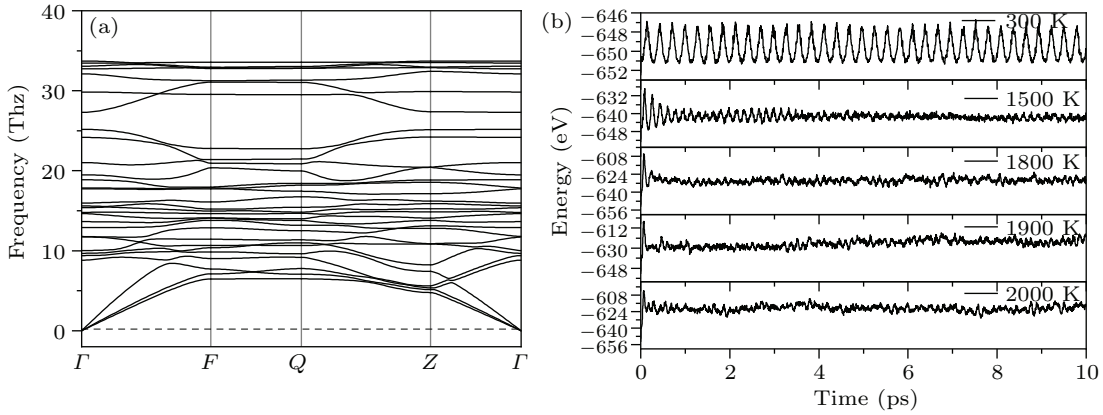


Fig. 4. (a) The phonon spectrum of *P*-1-VN_4 at atmosphere pressure. (b) The total energy of *P*-1-VN_4 in molecular dynamics simulation.

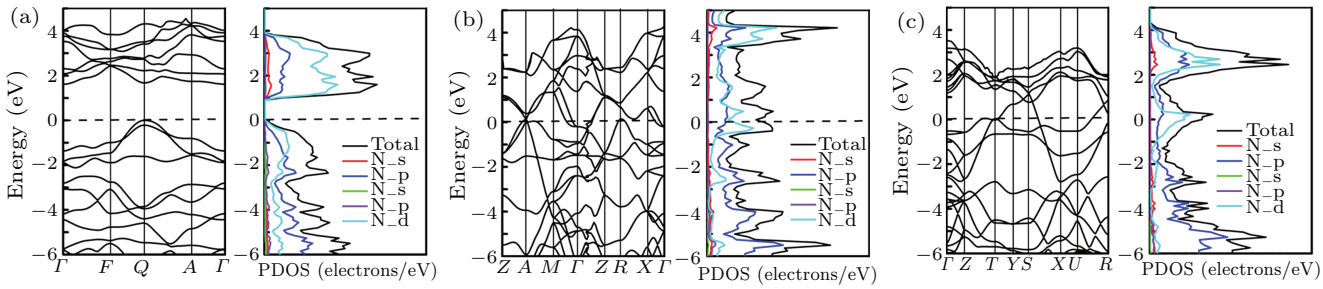


Fig. 5. Band structures and PDOS of (a) *P*-1-VN_4 at 100 GPa, (b) *P*4*mnc*-VN_8 at 100 GPa, and (c) *Immm*-VN_{10} phases at 50 GPa.

Moreover, the presented phonon dispersion curves in Fig. 4(a) shows that the *P*-1-VN_4 also possesses the dynamics stability at ambient pressure. The molecular dynamics simulations are performed to confirm the thermal stability of *P*-1-VN_4 at ambient pressure. As shown in Fig. 4(b) and Fig. S3, the *P*-1-VN_4 possesses the thermal stability up to 1500 K. For the temperature increases up to 1800 K, some N_4-chains are decomposed to the N_2 molecules. Further increase the temperature, some armchair N-chains began to decompose and form the new N_4-chain and N_6-chain structures. Finally, the decomposition of all the N_4-chains and armchair N-chains occurs with the temperature up to 2000 K. Thus, the *P*-1-VN_4 may be quenched to ambient conditions as the metastable phase.

As the armchair N-chain structures are formed in *P*-1-VN_4, *P*4*mnc*-VN_8, and *Immm*-VN_{10} phases, we performed the calculations of the band structures, projected density of states (PDOS), the electron localized function (ELF) and the Bader charge for further understanding their electronic structure and bonding property. For the presented band structure and PDOS in Fig. 5, we can see that the *P*-1-VN_4 is the semiconductor phase with the band gap of 0.95 eV, while the *P*4*mnc*-VN_8 and *Immm*-VN_{10} are the metal phases. The density of states near the Fermi level is almost contributed by the N_2p and V_d orbital electrons. For the presented ELF in Fig. 6, we can see that the N atoms in armchair N-chain structures are sp^2-hybridized due to the exhibited high localized state of electrons between the N atoms and lone electronic pairs at the corner. The formed N–N covalent bond plays an important role for the structural stability of N-chain. The average bond length in N-chain structure are 1.34, 1.29, and 1.28 Å in *P*-1-VN_4, *P*4*mnc*-VN_8, and *Immm*-VN_{10} phases, which are located between N=N double bond (1.25 Å) and N–N single bond (1.45 Å). In Table 3, the Bader charge analysis shows that the vanadium atom and nitrogen atom are the electron donor and the electron acceptor, respectively. The charge transformation quantity from each vanadium atom to the N-chain is approximately 1.57, 1.50, and 1.36 electrons for the *P*-1-VN_4, *P*4*mnc*-VN_8, and *Immm*-VN_{10} phases, respectively. This charge transfer results in a V–N ionic bond interaction, which further improves the stability of N-chain structure.

As is well known, the energy liberation of the polymeric nitrogen structure mainly originates from the recombination

of the N≡N bond after the decomposition of the N–N single-bond or N=N double-bond. The energy density and detonation properties of polymeric nitrogen are significantly sensitive to the nitrogen concentration and polymeric N-structure. The high nitrogen content with the armchair N-chain structure of *P*-1-VN_4, *P*4*mnc*-VN_8, and *Immm*-VN_{10} make them potential capacity as the high energy density materials (HEDMs). The energy density of VN_x compound was calculated at ambient pressure. The decompose reaction path is as follows: $VN_x \rightarrow V + xN_2$. The most stable *Fm*-3*m*-V and *Pa*-3-N_2 are selected as the decomposition products. The enthalpy of the VN_x compound is subtracted from the enthalpy of the V and N_2, and the unit (in unit eV) of the enthalpy difference is converted into kJ/g. As shown in Table 4, the energy densities of *P*-1-VN_4, *P*4*mnc*-VN_8, and *Immm*-VN_{10} are 0.79 kJ/g, 2.86 kJ/g, and 3.13 kJ/g, respectively. The detonation velocities and detonation pressures of *P*-1-VN_4, *P*4*mnc*-VN_8, and *Immm*-VN_{10} are (90.45 km/s, 11.68 GPa), (58.04 km/s, 10.67 GPa), and (135.05 km/s, 15.04 GPa), respectively. For the formed same N-chain structure, the relatively low energy density of *P*-1-VN_4 is due to its nitrogen content is lower than the *P*4*mnc*-VN_8 and *Immm*-VN_{10}. In comparison, the energy densities of *P*4*mnc*-VN_8 and *Immm*-VN_{10} are close to that of TNT. The detonation velocities of *P*-1-VN_4, *P*4*mnc*-VN_8, and *Immm*-VN_{10} are significantly larger than that of TNT, while the detonation pressures are also close to that of TNT. Thus, the outstanding detonation properties of *P*-1-VN_4, *P*4*mnc*-VN_8, and *Immm*-VN_{10} allow them as the potential application in explosive field.

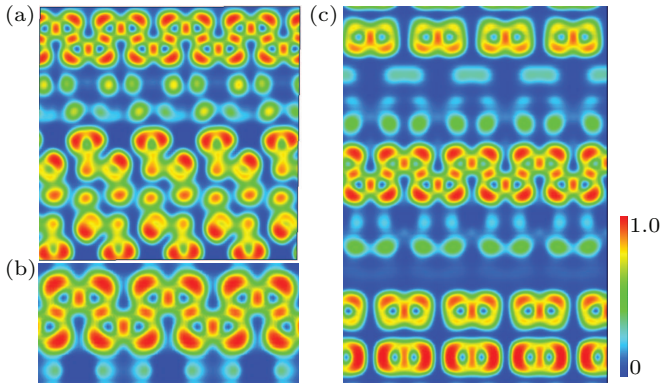


Fig. 6. The ELFs of (a) *P*-1-VN_4, (b) *P*4*mnc*-VN_8, and (c) *Immm*-VN_{10} phases.

Table 3. The Bader charge analysis of *Pnab*-V_2N, *Pnnm*-V_2N, *P*-6*m*2-VN, *I*4*mcm*-VN_2, *P*-1-VN_4, *P*4*mnc*-VN_8, *Immm*-VN_{10} at different pressures. The negative and positive values mean the donor and the acceptor of charge.

Structure	Pressure	Element	σ(e) (atom)
P-1-VN_4	100	V	+1.5653
		N	–0.3913
*P*4*mnc*-VN_8	100	V	+1.5043
		N	–0.1880
Immm-VN_{10}	50	V	+1.3587
		N	–0.13587

Table 4. The energy density and detonation properties of *P*-1-VN_4, *P*4*mnc*-VN_8, and *Immm*-VN_{10} are presented. The corresponding properties of TNT are presented for the comparison analysis.

Compunds	Energy densities (kJ/g)	Detonation velocity (km/s)	Detonation pressure (GPa)
P-1-VN_4	0.79	11.68	90.45
*P*4*mnc*-VN_8	2.86	10.67	58.04
Immm-VN_{10}	3.13	15.04	135.05
TNT	4.30[45]	6.90[54]	19.00[53]

4. Conclusions

The high-pressure study on V–N compounds is performed by using the particle swarm optimization methodology combined with first-principles calculations. As a result, we proposed seven stable high-pressure phases, for which the stable pressures ranges have been identified. The armchair N-chair structures are formed in N-rich structures of *P*-1-VN_4, *P*4*mnc*-VN_8, and *Immm*-VN_{10}. Moreover, the *P*-1-VN_4 may be quenched to ambient conditions as the metastable phase. The *P*-1-VN_4 is the semiconductor phase, while the *P*4*mnc*-VN_8 and *Immm*-VN_{10} are the metal phases. The N atoms in armchair N-chain structures are sp^2-hybridized and bonded with the adjacent ones with the covalent bond form, which plays an important role for the structural stability. This charge transfer results in a V–N ionic bond interaction, which further improves the stability of N-chain structure. The analysis of energy density and detonation properties shows that the *P*-1-VN_4, *P*4*mnc*-VN_8, and *Immm*-VN_{10} with the outstanding detonation properties have potential application in explosive field. This work not only enriches the high-pressure diagram of V–N system, but also provides the guidance of experimental synthesis in the future.

References

[1] Mattson W D, Sanchez-Portal D, Chiesa S and Martin R M 2004 *Phys. Rev. Lett.* **93** 125501
[2] Liang D M, Liu H Y, Gan Y D, Kuang A L and Tian C L 2021 *Chin. Sci. Bull.* **66** 2908
[3] Hirshberg B, Gerber R B and Krylov A I 2014 *Nat. Chem.* **6** 52
[4] Lang Q, Sun Q, Xu Y G, Wang P C, Lin Q H and Lu M 2021 *New J. Chem.* **45** 6379
[5] Alemany M M G and Martins J. L 2003 *Phys. Rev. B* **68** 241101
[6] Zahariev F, Hu A, Hooper J, Zhang F and Woo T 2005 *Phys. Rev. B* **72** 214108
[7] Hu A G, Zhang F and Woo T 2010 *Phys. Rev. B* **82** 125410
[8] Wang X L, He Z, Ma Y M, Cui T, Liu Z M, Liu B B, Li J F and Zou G T 2007 *J. Phys.: Condens. Matter* **19** 425226
[9] Zahariev F, Hooper J, Alavi S, Zhang F and Woo T K 2007 *Phys. Rev. B* **75** 140101
[10] Ma Y M, Oganov A R, Li Z W, Xie Y and Kotakoski J 2009 *Phys. Rev. Lett.* **102** 065501
[11] Wang X L, Tian F B, Wang L C, Cui T, Liu B B and Zou G T 2010 *J. Chem. Phys.* **132** 024502
[12] Sun M, Yin Y H and Pang Z K 2015 *Comput. Mater. Sci.* **98** 399
[13] Wang X L, Wang Y C, Miao M S, Zhong X, Lv J, Cui T, Li J F, Chen L, Pickard C J and Ma Y 2012 *Phys. Rev. Lett.* **109** 175502
[14] Eremets M I, Gavriliuk A G, Trojan I A, Dzivenko D A and Boehler R 2004 *Nat. Mater.* **3** 558

[15] Laniel D, Winkler B, Fedotenko T, Pakhomova A, Chariton S, Milman V, Prakapenka V, Dubrovinsky L and Dubrovinskaia N 2020 *Phys. Rev. Lett.* **124** 216001

[16] Tomasino D, Kim M, Smith J and Yoo C S 2014 *Phys. Rev. Lett.* **113** 205502

[17] Laniel D, Geneste G, Weck G, Mezouar M and Loubeyre P 2019 *Phys. Rev. Lett.* **122** 066001

[18] Zhang S T, Zhao Z Y, Liu L L and Yang G C 2017 *J. Power Sources* **365** 155

[19] Wei S L, Li D, Liu Z, Wang W, Tian F B, Bao K, Duan D F, Liu B B and Cui T 2017 *J. Phys. Chem. C* **121** 9766

[20] Wei S L, Li D, Liu Z, Li X, Tian F B, Duan D F, Liu B B and Cui T 2017 *Phys. Chem. Chem. Phys.* **19** 9246

[21] Zhu S S, Peng F, Liu H Y, Majumdar A, Gao T and Yao Y S 2016 *Inorg. Chem.* **55** 7550

[22] Yu S Y, Huang B, Zeng Q F, Oganov A R, Zhang L T and Frapper G 2017 *J. Phys. Chem. C* **121** 11037

[23] Zhu W H, Xu X J and Xiao H M 2007 *J. Phys. Chem. Solids* **68** 1762

[24] Li L, Kuo B, Xingbing Z and Tian C 2021 *J. Phys. Chem. C* **125** 24605

[25] Zhang J, Zeng Z, Lin H Q and Li Y L 2014 *Sci. Rep.* **4** 4358

[26] Wang X L, Li J F, Xu N, Zhu H Y, Hu Z Y and Chen L 2015 *Sci. Rep.* **5** 16677

[27] Zhang M G, Yan H Y, Wei Q, Wang H and Wu Z J 2013 *Europhys. Lett.* **101** 26004

[28] Prasad D L V K, Ashcroft N W and Hoffmann R 2013 *J. Phys. Chem. C* **117** 20838

[29] Ramesh Babu K and Vaitheeswaran G 2013 *Chem. Phys. Lett.* **586** 44

[30] Steele B A, Stavrou E, Crowhurst J C, Zaug J M, Prakapenka V B and Oleynik I I 2017 *Chem. Mater.* **29** 735

[31] Steele B A and Oleynik I I 2016 *Chem. Phys. Lett.* **643** 21

[32] Peng F, Han Y X, Liu H Y and Yao Y S 2015 *Sci. Rep.* **5** 16902

[33] Peng F, Yao Y S, Liu H Y and Ma Y M 2015 *J. Phys. Chem. Lett.* **6** 2363

[34] Bykov M, Bykova E, Koemets E, Fedotenko T, Aprilis G, Glazyrin K, Liermann H P, Ponomareva A V, Tidholm J, Tasnadi F, Abrikosov I A, Dubrovinskaia N and Dubrovinsky L 2018 *Angew. Chem. Int. Ed.* **57** 9048

[35] Huang B and Frapper G 2018 *Chem. Mater.* **30** 7623

[36] Xia K, Gao H, Liu C, Yuan J N, Sun J, Wang H T and Xing D Y 2018 *Sci. Bull.* **63** 817

[37] Wei Q, Zhao C Y, Zhang M G, Yan H Y and Wei B 2019 *Phys. Lett. A* **383** 2429

[38] Steele B A and Oleynik I I 2017 *J. Phys. Chem. A* **121** 8955

[39] Liu S, Liu R, Li H Y, Yao Z, Shi X H, Wang P and Liu B B 2021 *Inorg. Chem.* **60** 14022

[40] Niu S F, Li Z H, Li H Y, Shi X H, Yao Z and Liu B B 2021 *Inorg. Chem.* **60** 6772

[41] Wei S L, Liu Z P, Guo Y H, Sun H Y, Chang Q and Sun Y P 2021 *J. Phys.: Condens. Matter* **33** 475401

[42] Li Y W, Feng X L, Liu H Y, Hao J, Redfern S A T, Lei W W, Liu D and Ma Y Y 2018 *Nat. Commun.* **9** 1

[43] Steele B A, Stavrous E, Prakapenka V B, Radousky H B, Zaug J M, Crowhurst J C and Oleynik I I 2015 *Cesium Pentazolate: a New Nitrogen-rich Energetic Material*, USA

[44] Laniel D, Weck G, Gaiffe G, Garbarino G and Loubeyre P 2018 *J. Phys. Chem. Lett.* **9** 1600

[45] Huifang D, Yangfeng G, Jinlong Z, Wei G and Yugui Y 2021 *Phys. Chem. Chem. Phys.* **23** 12350

[46] Huifang D and Wei G 2022 *J. Phys. Conden. Matter* **34** 235702

[47] Chuli S, Wei G and Yugui Y 2022 *Chin. Phys. Lett.* **39** 087101

[48] Zhang J, Oganov A R, Li X F and Niu H Y 2017 *Phys. Rev. B* **95** 020103

[49] Bykov M, Bykova E, Aprilis G, Glazyrin K, Koemets E, Chuvashova I, Kupenko I, McCammon C, Mezouar M, Prakapenka V, Liermann H P, Tasnádi F, Ponomareva A V, Abrikosov I A, Dubrovinskaia N and Dubrovinsky L 2018 *Nat. Commun.* **9** 2756

[50] Yu R M, Sun Ermiao, Jiao L G, Cai Y M, Wang H B and Yao Y S 2018 *RSC Adv.* **8** 36412

[51] Yanchao W, Jian L, Li Z and Yanming M 2012 *Comput. Phys. Commun.* **183** 2063

[52] John P P, Kieron B and Matthias E 1996 *Phys. Rev. Lett.* **77** 3865

[53] Kamlet M J and Dickinson C 1968 *J. Chem. Phys.* **48** 43

[54] Agrawal J P 2010 *High Energy Materials: Propellants, Explosives and Pyrotechnics* (John Wiley & Sons)